Lanthanide-Binding Lanmodulin-Based Peptides: Insights from Advanced Mass Spectrometry Techniques

Sophie M. Gutenthaler-Tietze, Lena J. Daumann, Patrick Weis

EurJIC
European Journal of Inorganic Chemistry

Research Article
doi.org/10.1002/ejic.202500258

Chemistry Europe
European Chemical Societies Publishing

www.eurjic.org

Lanthanide-Binding Lanmodulin-Based Peptides: Insights from Advanced Mass Spectrometry Techniques

Sophie M. Gutenthaler-Tietze, Lena J. Daumann,* and Patrick Weis*

Selective peptide ligands for lanthanides (Ln) have multiple applications in, for example, Ln-separation and recycling or as lanthanide-binding tags. Optimizing peptides for Ln-binding can be cumbersome and many techniques need high sample volumes. Here short 12-aminoacid peptides are investigated based on the metal-binding loops of the natural Ln-binding protein lanmodulin with advanced gas-phase techniques such as ion mobility spectrometry, collision-induced dissociation, and electrospray ionization to gain insight into binding residues and possible differences between sequences. Both the natural sequences as well as peptides that are synthesized in "reverse" order are investigated and it is found that the trends observed in solution measurements are well reproduced by gas-phase measurements.

1. Introduction

Lanthanides (Ln) are critical elements for our modern life as they are widely used in catalysis, imaging, and therapeutic applications due to their unique electronic properties.[1] About a decade ago it was established that bacteria also use Ln in their metabolism sparking a new field.[2] In 2018 the first natural Ln-binding protein, lanmodulin (LanM), was isolated from *Methylobacterium extorquens* AM1. Lanmodulin belongs to the class of EF-hand proteins and possesses four 12-amino acid long binding loops of which three exhibit a picomolar affinity to Lns.[3] We recently investigated all four 12-amino acid long binding loops as synthesized peptides in their native sequence[4] as well as "reversed", that is, synthesized the other way around (see **Figure 1**).[5] The peptides following the native sequence had Eu^{3+} and Tb^{3+} affinities in the low micromolar range (around 5 μM) while three out of four of the reversed peptides established Ln-affinities around 500 nM. Thus, by reversing nature's sequence the affinity was increased by one order of magnitude. Only for EF4 and EF4-R no significant differences between the observed Ln-affinities could be determined.[4,5] We previously used a combination of nuclear magnetic resonance (NMR) spectroscopy, isothermal titration calorimetry (ITC), circular dichroism (CD), and time-resolved laser fluorescence spectroscopy (TRLFS) to gain insight into the binding of Ln to the peptides in solution. For these measurements high quantities of the peptides as well as time-intensive experiments and data analysis are needed.

The study of peptide-lanthanide binding interactions through advanced gas-phase techniques such as ion mobility spectrometry (IMS), collision-induced dissociation (CID), and electrospray ionization (ESI) mass spectrometry provides insights into their coordination chemistry in the gas phase and could be an attractive tool for a quick assessment of the coordination, selectivity, and (partially, also) stability of peptide-Ln complexes. IMS in combination with mass spectrometry is a technique to separate isomers and identify structures of ions in gas phase that dates back more than 30 years. Since then it has been widely applied to biomolecules such as oligonucleotides, sugars, proteins, and peptides.[6–9] Here we compare the four 12-amino acid EF-hand peptides from LanM synthesized in forward and reverse sequence with free N-terminus and C-terminus in gas-phase measurements with Eu. This lanthanide was chosen to complement the previously reported experiments in solution of which a majority was performed with Eu.[4,5] To the best of our knowledge this is the first study investigating Ln-binding peptides in the metal-bound state using this combination to ultimately advance our understanding of how peptides can be optimized for selective Ln binding in solution-phase environments.

2. Results and Discussion

2.1. ESI Mass Spectra of Different Peptides

We first started our investigations by focusing on studying the native and reversed peptide sequences using mass spectrometry methods based on electrospray ionization techniques. Hereby, the predominant charge states of the formed ions were 2+ and 3+, either doubly and triply protonated or with up to three

S. M. Gutenthaler-Tietze, L. J. Daumann
Chair of Bioinorganic Chemistry
Heinrich-Heine-Universität
Universitätsstraße 1, 40225 Düsseldorf, Germany
E-mail: lena.daumann@hhu.de

P. Weis
Institute for Physical Chemistry II
Karlsruher Institut für Technologie
Fritz-Haber Weg 2, 76131 Karlsruhe, Germany
E-mail: Patrick.weis@kit.edu

Supporting information for this article is available on the WWW under https://doi.org/10.1002/ejic.202500258

Research Article
doi.org/10.1002/ejic.202500258

Chemistry Europe
European Chemical Societies Publishing

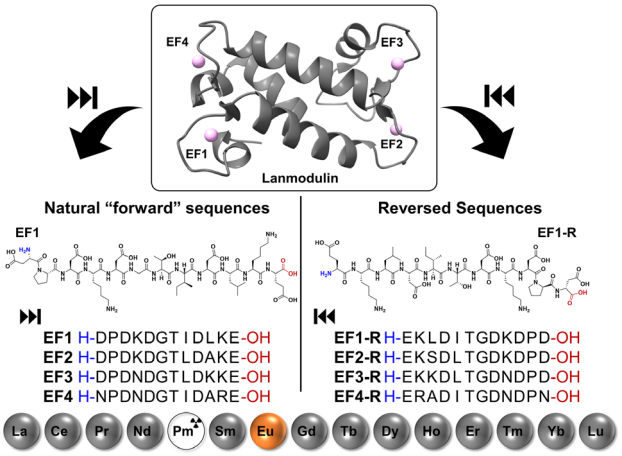

Figure 1. Structure of lanmodulin with bound neodymium (PDB:8fns[18]) and the sequences of the lanmodulin-inspired peptides following the natural sequence on the right and synthesized in reverse order on the left; all peptides are shown from N to C-terminus.

Eu^{3+} ions (each replacing three protons). In **Figure 2** the ESI mass spectra (obtained with a Waters instrument) of the isomeric peptides EF1 and EF1-R in the 10:50 μM mixture with $EuCl_3$ are shown. The corresponding mass spectra of the other peptide-$EuCl_3$ mixtures (see Figure 1 for the sequences of all tested peptides) are similar and included in the supporting information (S1–S3). The relative intensities of the complexes with Eu^{3+} vs. protonated peptides vary slightly from peptide to peptide, but in all cases the different Eu^{3+} complexes can be easily identified in high intensities. Besides the formation of 1:1 peptide to Eu^{3+} complexes, the formation of 1:2 peptide to Eu^{3+} complexes was not surprising, as we have previously observed both 1:1 and 1:2 peptide:Eu^{3+} complexes in solution by means of ITC, TRLFS and NMR spectroscopy.[4,5] The 1:3 complex was, however, so far only observed in the gas phase as minor species.

2.2. Collision Induced Dissociation

In order to shed more light into the structure, stability, and fragmentation channels of the different complexes we performed CID in a LTQ XL Orbitrap mass spectrometer on the different isolated species as shown in **Figure 3** and S4–S14, Supporting Information. The great advantage of CID measurements is that they are usually available at mass spectrometry facilities and thus guarantee rapid insights.

For CID, the respective ions are mass selected in the ion trap of the instrument, then excited for 30 ms with an excitation energy of 18–19 NCE (NCE = normalized collision energy, i.e., instrument specific units) for dications and 12 NCE for tricationts. Under these conditions all species undergo significant fragmentation, but the precursor ion remains detectable. The resulting fragment ions are transferred for high-resolution mass analysis ($R > 150\,000$) into the orbitrap cell. We first focused on the 2+ charge state and compared the fragmentation patterns of the doubly protonated peptides with the respective complexes with europium (in the same charge state, i.e., three protons replaced by one Eu^{3+} ion). The protonated peptides show the expected typical peptide fragmentation patterns,[11,12] i.e., fragmentation into smaller peptide ions by cleavage of one of the various peptide bonds (b- and y-fragment ions[13]), see Figure 3a for $[EF1 + 2H]^{2+}$ and **Figure 4**a for a graphical representation. However, the

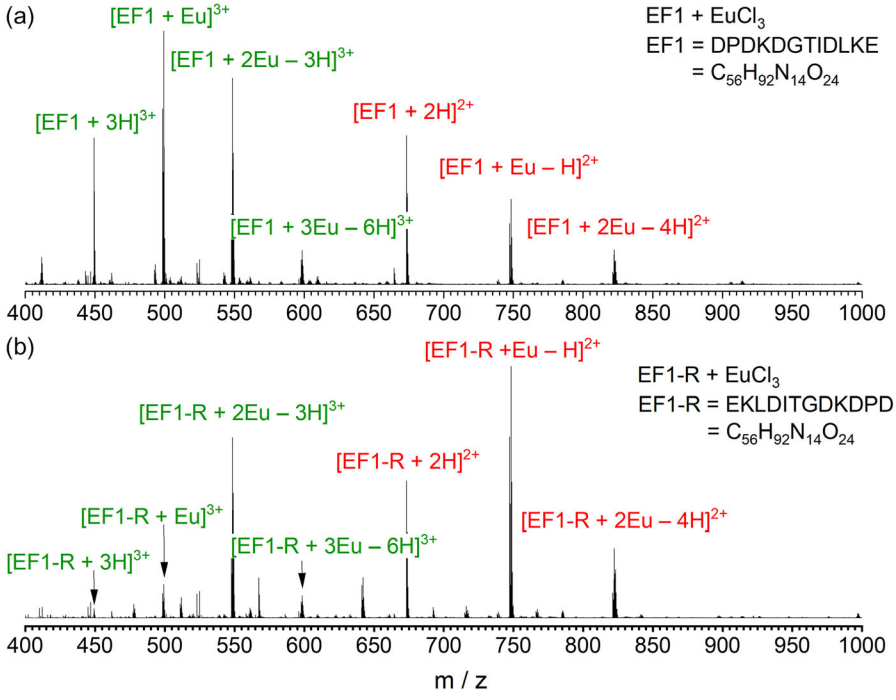

Figure 2. a) ESI (positive mode) mass spectra of mixtures of 10 μM EF1 and 50 μM $EuCl_3$ in water. b) 10 μM EF1-R and 50 μM $EuCl_3$ in water. Doubly charged species are shown in red and triply charged species in green.

Research Article
doi.org/10.1002/ejic.202500258

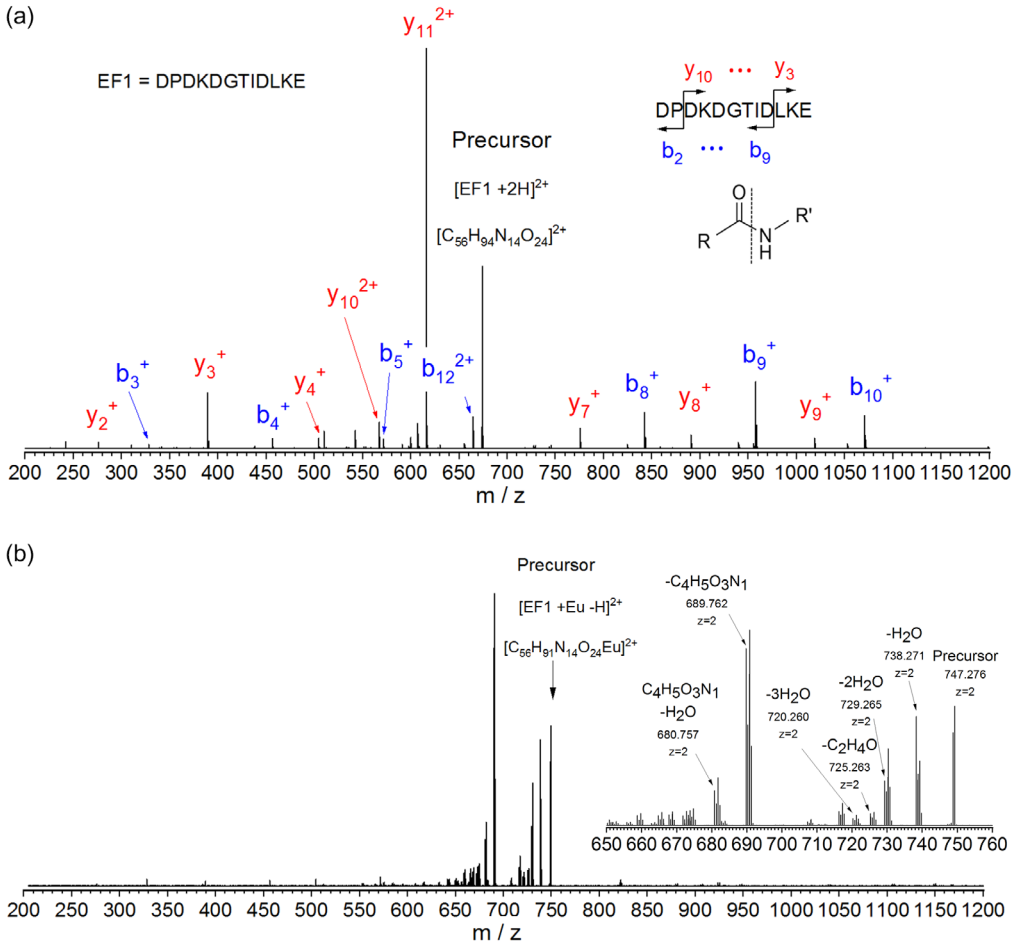

Figure 3. a) Collision-induced dissociation (CID) of $[EF1 + 2H]^{2+}$. The used nomenclature for the obtained fragments is exemplary shown with the inserted sequence. b) CID of $[EF1 + Eu - H]^{2+}$. The masses in the enlarged insert correspond to the respective monoisotopic masses. Identical activation parameters, that is, excitation time width 30 ms, energy 18 NCE. The masses correspond to the monoisotopic peaks, calculation and experiment agree to within 5 ppm or better. The calculated and measured mass differences between precursor and fragment ions are within 1 ppm or better.

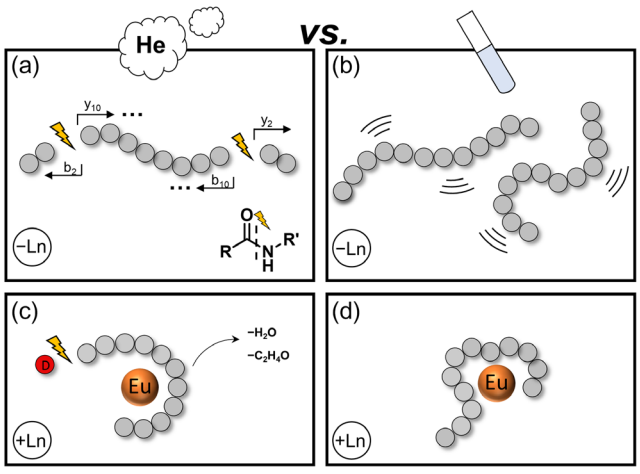

Figure 4. Simplified graphical depiction of the different behavior of the peptides in the gas phase versus in aqueous solution highlighting in a) the typical fragmentation pattern of the metal free peptides in the gas phase and in b) the high structural dynamic in aqueous solution. In c) the schematic fragmentation pattern in the gas phase is shown for $[EFX + Eu - H]^{2+}$ ($X = 1$–3), while the formed complex in solution is shown in (d).

corresponding Eu-containing ions $[EF1 + Eu - H]^{2+}$ (three protons replaced by one Eu^{3+} ion) show a completely different fragmentation pattern, dominated by the loss of small neutral molecules such as water, $C_4H_5O_3N$ and C_2H_4O, see Figure 3b. The typical peptide fragmentation pattern cannot be observed. Very similar observations can also be made for EF2 and EF3 for which the loss of $C_4H_5O_3N$ ($m = 115.027$) is also the dominant fragmentation channel (or at least at comparable intensity as water loss). This fragment can most likely be attributed to the cleavage of the N-terminal aspartic acid while the observed C_2H_4O fragment can tentatively be assigned as the loss of acetaldehyde from the threonine side-chain.[14,15] See Figure 4a for a graphical representation.

This unusual fragmentation behavior is in principle similar for the other investigated peptide-Eu^{3+} complexes, (peptides = EF1-R, EF2-R, EF3-R, EF4, and EF4-R), see supporting information S4–S10. However, there are some differences when looking at the different peptides in detail. For example, the fragment mass spectra of the reversed peptides $[EFX-R + Eu - H]^{2+}$ ($X = 1$–4) are dominated by loss of one and two (neutral) water molecules. And interestingly the loss of a $C_4H_5O_3N$ fragment is absent or at much smaller intensity. We tentatively explain this finding (the reduction of the

fragmentation of Eu-bound vs free peptide) with the following simple picture: The peptides wrap around the triply charged metal center and are stabilized by additional bonding interactions, especially between several of the oxygen atoms of the peptide and the Eu^{3+} center. In this case, cleavage of one of the peptide bonds is not sufficient to observe fragmentation since the two respective fragment ion moieties might still be held together via the metal ion. Instead, rearrangement leading to water loss is the dominant fragment channel in most cases. However, as already mentioned above, the peptides EF1, EF2, and EF3 fall out of line as the loss of neutral $C_4H_5O_3N$ (most probably cleavage of the N-terminal aspartic acid) is as an important fragmentation channel as the loss of water. In contrast to that, the loss of glutamic acid from the C-terminus is not observed for these peptides in significant amounts (see Figure 3, S5, and S7, Supporting Information). A possible explanation for this is that in EF1, EF2, and EF3 the N-terminal aspartic acid is not directly bound to the Eu^{3+} metal center and therefore cleavage of the peptide bond to the remaining peptide is sufficient to observe the fragment ion while the C-terminal glutamic acid is stabilized by an additional bond to the Eu^{3+} and therefore not observed as a fragment ion. This hypothesis perfectly aligns with observations made for the forward peptides in solution. For all three peptides MD simulations suggested previously that the N-terminal aspartic acid is facing away from the coordinating Eu^{3+}, while the C-terminal glutamic acid is involved in binding.[4,5] By NMR studies with EF1 these observations were also recently confirmed.[5] This means that CID measurements hold the potential to indicate whether, for example, terminal amino acids are involved in metal-binding or not, thus giving important structural insights.

As mentioned above for the corresponding reverse peptides EF1-R, EF2-R, and EF3-R neither loss of aspartic acid from the C-terminus nor loss of glutamic acid from the N-terminus is a significant channel compared to the dominant water loss (see Figure S4, S6, and S8, Supporting Information). This might support the observations from studies in solution that the reverse peptides have a higher Ln-affinity and form more stable complexes and therefore presents the possibility to gain such insights more quickly.[5] For the peptide EF4 ($[EF4+Eu\text{-}H]^{2+}$), the only sequence with asparagine at the N-terminus, we observe the most complicated fragmentation mass spectrum, with (multiple) H_2O, C_2H_4O, and $C_4H_6O_2N_2$ loss as well as some backbone fragmentation at low intensity (see Figure S9b, Supporting Information). While the loss of C_2H_4O can again be assigned to the threonine sidechain,[14,15] the loss of $C_4H_6O_2N_2$ corresponds to a potential cleavage of asparagine. In comparison, for EF4-R, the only peptide with a C-terminal asparagine, we solely observe the loss of water, similarly to the residual reverse peptides as discussed before.

For the peptide-Eu^{3+}complexes in charge state 3+ the CID data are shown in Figure S11–S14, Supporting Information. Again the dominant fragmentation channel is loss of small neutral molecules such as water and C_2H_4O (potentially acetaldehyde from the threonine sidechain[14,15]). Peptide bond cleavage is only observed as a minor fragmentation channel resulting in small singly and larger doubly charged fragments (with the Eu^{3+} bound to the doubly charged fragment), see Figure S13, Supporting Information as example.

To summarize the CID measurements, metallation of the peptide by Eu^{3+} leads to dramatic changes in fragmentation patterns, dominated by water loss in case of the reverse peptides and the additional loss of the N-terminal amino acid in case of the native forward sequences. We explain this behavior by compact structures with the peptide wrapped around and stabilized by the metal centers (see Figure 4).

2.3. Ion Mobility Measurements

To not only investigate the fragmentation but to shed some more light onto the structures of the peptides with and without Eu^{3+} we performed ion mobility measurements (IMS) of the different isolated species (see **Figure 5**). Gas-phase ion mobility spectrometry is a very sensitive tool to identify and separate isomeric ions by differences in their collision cross sections (CCS).

It has been used in peptide mass spectrometry for more than 30 years[6–10] and since two decades commercial instruments are available, such as the Synapt G2 and Agilent 6560. By comparing with theoretical CCS obtained via trajectory calculations for candidate structures based on molecular dynamic simulations or quantum chemical calculations even a quantitative structural assignment is possible. Qualitatively, for a given charge state compact, folded structures have smaller cross sections than open, unfolded structures. Therefore, IMS can give important structural insights on the formed peptide-metal complexes.

Figure 5 shows the "mobilograms" (intensity vs CCS) for EF1 and EF1-R with 0,1, and 2 Eu^{3+} counterions (each replacing three protons) in charge states 2+ and 3+.

For the protonated trications $[EF1 + 3H]^{3+}$ and $[EF1\text{-}R + 3H]^{3+}$ we observe a single peak for each species corresponding to CCS of 494 and 490 Å^2, respectively (see Figure 5a). The protonated dications $[EF1 + 2H]^{2+}$ and $[EF1\text{-}R + 2H]^{2+}$ have much smaller CCS of 394 and 386 Å^2 (see Figure 5b). The larger CCS for charge state 3+ is due to the increased Coulomb repulsion which leads to unfolding of the peptide ion in gas phase, while in the lower charge state 2+ the van-der-Waals interactions lead to more compact, "folded" structures. Unfolding of peptide ions with increasing charge state is well known in gas phase.[6] The peak widths of the mobilograms of $[EF1 + 3H]^{3+}$(Figure 5a), $[EF1 + 2H]^{2+}$ and $[EF1\text{-}R + 2H]^{2+}$ (Figure 5b) are very narrow and close to the experimental resolution, which implies that basically one conformer, or at least a very narrow conformer distribution is present in these cases. The peak width for the triply protonated reverse peptide $[EF1\text{-}R + 3H]^{3+}$ is slightly larger with a tailing to larger CCS (see Figure 5a). This implies the presence of at least two isomers with slightly different CCS. The Eu-containing trications $[EF1 + Eu]^{3+}$ and $[EF1\text{-}R + Eu]^{3+}$ have CCS of 439 and 436 Å^2 (Figure 5c), that is, replacement of the three extra protons by one Eu^{3+} ion leads to a dramatic CCS decrease of around 55 Å^2. In line with our CID experiments (and previous experiments in solution[4,5]) we explain this finding with the peptide wrapping around the metal center. On the contrary, the dications

Research Article
doi.org/10.1002/ejic.202500258

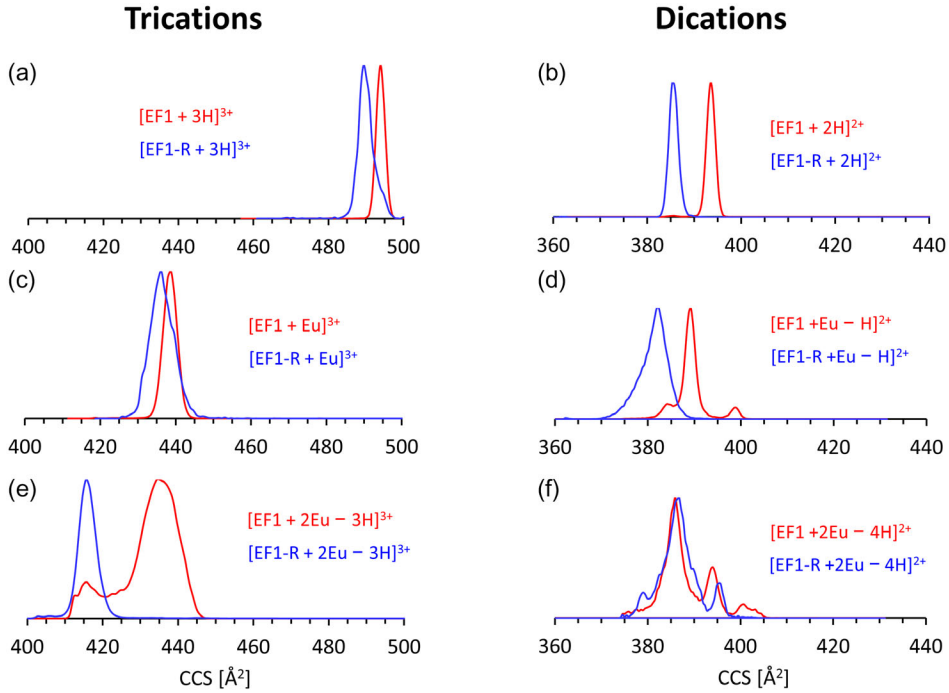

Figure 5. Mobilograms of EF1 (in red) and EF1-R (blue) complexes in different charge states and Eu^{3+} coordination states. Panels (a,c, and e) show complexes in 3+ charge state with (a) 0, (c) 1 and (e) 2 Eu^{3+} counterions. Panels (b,d, and f) show complexes in the 2+ charge state with (b) 0, (d) 1 and (f) 2 Eu^{3+} counterions.

$[EF1 + Eu - H]^{2+}$ and $[EF1\text{-}R + Eu - H]^{2+}$ have CCS (389 and 382 $Å^2$ Figure 5d) that are similar to the respective protonated species $[EF1 + 2H]^{2+}$ and $[EF1\text{-}R + 2H]^{2+}$ (only 5 $Å^2$ smaller, see Figure 5d vs. b). This can be easily explained by the fact that the doubly protonated species $[EF1 + 2H]^{2+}$ and $[EF1\text{-}R + 2H]^{2+}$ are already folded to compact conformations, even without the presence of a Eu^{3+} counterion. Therefore, the replacing of protons by Eu^{3+} does lead to a large CCS change. For the trications, the second Eu^{3+} does not change the CCS as dramatically as the first (see Figure 5e), which is probably because the structure is already very compact. It should be noted that the Eu-containing species have broader, more structured mobilograms than the protonated peptides, indicating that several isomers are present that are not (or at least slowly) interconverting on the timescale of the ion mobility measurement (100–200 ms). The same holds true for dicationic species with two Eu^{3+} centers (Figure 5f). For the other peptides EF2, EF3, EF4, and the corresponding reverse peptides EF2-R, EF-3-R, EF4-R the trends observed for EF1 and EF1-R are confirmed, that is, the compaction by proton replacement by Eu^{3+} and the observation of several isomers (see **Table 1** and S1 and Figures S15–S17, Supporting Information).

So, if available, IMS can provide additional information about the conformer/isomer distribution of formed peptide-metal complexes and shows the folding/unfolding dynamics as function of charge state and sequence. If IMS is used in combination with predictions from theory, these structural assignments can even be put on a more quantitative basis, making IMS an interesting tool for the investigation of metal-binding peptides.

Table 1. CCS (in $Å^2$) for the "native" peptides and metal complexes as identified from the peak positions in Figure 5 and S15-S17, Supporting Information. The statistical error is 2 $Å^2$. In brackets the intensity (in %) of the respective isomer.

	EF1	EF2	EF3	EF4
$[EFX + 3H]^{3+}$	494(100)	488 (100)	475 (95) 481 (5)	482 (100)
$[EFX + Eu]^{3+}$	439(100)	432 (100)	434 (100)	446 (100)
$[EFX + 2Eu - 3H]^{3+}$	435 (80) 416 (20)	430 (90) 410 (10)	419 (100)	421 (100)
$[EFX + 2H]^{2+}$	393(100)	387 (100)	390 (10) 393 (90)	380 (100)
$[EFX + Eu - H]^{2+}$	384 (13) 389 (82) 399 (7)	380(81) 385(16) 396(3)	385 (70) 388 (30)	379 (100)
$[EFX + 2Eu - 4H]^{2+}$	385 (72) 394 (13) 400 (8)	376 (76) 381 (30) 389 (8) 395 (6)	383 (25) 394 (75)	382 (22) 397 (78)

3. Conclusion

While gas phase and solution phase do not necessarily give rise to the same species and species distribution, some of the trends we have observed for the different peptides in solution are well reflected the measurements in the gas phase. This could contribute to the rapid identification of some binding residues involved and peptides that are optimal for binding metal ions through fast screening of larger peptide libraries. Especially, diversifying the position of coordinating amino acids in a peptide chain while

leaving the number of potentially coordinating sites the same, in combination with CID measurements, could allow for quick identification of differences in metal-binding ability (e.g., involvement of C-terminal amino acids) of larger peptide libraries. While not all facilities will have access to IMS, the CID measurements that can be done on standard MS instruments, provided in our study a good indicator of stability, and some information on the residues involved in binding though characteristic fragmentation patterns. In our small library, the matching reverse and forward peptides contained the same number of carboxylates. The behavior in the gas phase demonstrated that the involvement of the C-terminus can be hugely different and this conclusion can be drawn without much sample needed (opposed to mg needed for NMR measurements) just from CID measurements and examining fragmentation patterns. If available, IMS provides additional information about the conformer/isomer distribution and folding/unfolding dynamics as function of charge state and sequence: For a given charge state, compact, folded structures have smaller cross sections than open, unfolded structures. By comparing with predictions from theory, these structural assignments can be put on a more quantitative basis. All in all, mass spectrometry methods can offer useful, and above all, fast insights into the binding behavior of Ln-binding peptides.

4. Experimental Section

Materials and Methods

All peptide samples were prepared in ultrapure water (type 1, pH 5.6, 18.2 MΩ cm at 25 °C). For this demineralised water was further purified using a Synergy UV system from Merck Millipore. $EuCl_3{\cdot}6H_2O$ was obtained from Sigma Aldrich at 99.99% trace metal basis and used as supplied. In this study, solely peptides previously[4,5] reported were used. Accordingly, the synthesis, purification and concentration determination of EF1, EF2, EF3, EF4, EF1-R, EF2-R, and EF3-R are described in detail elsewhere[4,5] and not repeated here. EF4-R was purchased from GenScript and the corresponding analytical data has been reported previously.[5] For all experiments peptide stock solutions in water were used. These stock solutions were stored at −80 °C until usage. For $EuCl_3$ 10 mM stock solutions were prepared in water and stored at −20 °C until usage. All samples for mass spectrometry measurements were prepared in water, with final concentrations of 10 μM of the respective peptide and 50 μM $EuCl_3$.

Mass Spectrometry

Ion mobility spectrometry mass spectrometry experiments were performed on a Waters Select Series Cyclic IMS. A schematic set-up for the Waters Select Series Cyclic IMS can be found in the literature.[16] The Waters Select Series Cyclic IMS combines a high-resolution time-of-flight mass spectrometer with a high-resolution cyclic ion mobility cell and a quadrupole mass filter prior to the cell. In the ion mobility cell mass selected ion packets are confined by a RF-electrical field in 1.8 mbar of nitrogen and propagated by periodic voltage pulses ("travelling wave", TW). The effective drift length of the instrument can be adjusted by keeping the ion packed in the cell for several cycles, depending on the required ion mobility resolution. Here, 5 cycles that correspond to a drift length of ≈5 m which is sufficient to resolve CCS differences of around 0.5% were used. The measured drift times depend on charge and shape of the ions and instrumental parameters such as nitrogen pressure, TW-height and -speed. Device-independent CCS were obtained by comparing the measured drift times with drift times of a set of calibrant ions with known CCS. For this calibration the Agilent tunemix (G1969-8500) and the data of Stow et al. were used.[17] Collision induced dissociation experiments were performed with a Thermo Fisher Scientific LTQ Orbitrap XL mass spectrometer by resonant radio frequency voltage (RF) excitation in the linear ion trap filled with $\approx 4{\cdot}10^{-3}$ mbar of He. All mass experiments were performed in positive ion mode using electrospray ionization (ESI). Data analysis was performed with Thermo Fisher Scientific Xcalibur version 4.0 and Waters Masslynx version 4.2 as well as Origin Lab OriginPro 2021. Fragment masses were calculated using the Fragment Ion Calculator provided by the Institute for Systems Biology, (http://db.systemsbiology.net/proteomicsToolkit/FragIonServlet.html).

Acknowledgements

P.W. and L.J.D. acknowledge the financial support from the Deutsche Forschungsgemeinschaft (DFG, German Research Foundation) through the Collaborative Research Centre "4f for Future" (CRC 1573, project number 471424360, project A02). Additionally, P.W. is grateful to KIT, Land B.-W. and DFG for the funding of a Waters Cyclic IMS system under Art. 91b GG. S.M.G.-T. thanks the Studienstiftung des Deutschen Volkes for funding through a doctoral scholarship.

Open Access funding enabled and organized by Projekt DEAL.

Conflict of Interest

The authors declare no conflict of interest.

Data Availability Statement

The data that support the findings of this study are available in the supplementary material of this article. Raw data underlying the results of this study are openly available in the RADAR4Chem repository at https://doi.org/10.22000/ffagf4wz475p163v.

Keywords: ion mobility · lanmodulin · lanthanides · mass spectrometry · peptides

[1] T. Cheisson, E. J. Schelter, *Science* **2019**, *363*, 489.
[2] L. J. Daumann, *Angew. Chem. Int. Ed.* **2019**, *58*, 12795.
[3] J. A. Cotruvo Jr., E. R. Featherston, J. A. Mattocks, J. V. Ho, T. N. Laremore, *J. Am. Chem. Soc.* **2018**, *140*, 15056.
[4] S. M. Gutenthaler, S. Tsushima, R. Steudtner, M. Gailer, A. Hoffmann-Röder, B. Drobot, L. J. Daumann, *Inorg. Chem. Front.* **2022**, *9*, 4009.
[5] S. M. Gutenthaler-Tietze, J. Kretzschmar, S. Tsushima, R. Steudtner, B. Drobot, L. J. Daumann, *ChemRxiv* **2024**.
[6] D. E. Clemmer, R. R. Hudgins, M. F. Jarrold, *J. Am. Chem. Soc.* **1995**, *117*, 10141.
[7] G. von Helden, T. Wyttenbach, M. T. Bowers, *Science* **1995**, *267*, 1483.
[8] T. Wyttenbach, G. von Helden, M. T. Bowers, *J. Am. Chem. Soc.* **1996**, *118*, 8355.
[9] E. Christofi, P. Barran, *Chem. Rev.* **2023**, *123*, 2902.

[10] M. Keng, K. M. Merz Jr., *J. Am. Soc. Mass Spectrom.* **2025**, https://doi.org/10.1021/jasms.5c00078.
[11] J. H. Gross, *Mass Spectrometry: A Textbook*, Springer, Berlin, Heidelberg **2004**.
[12] R. Aebersold, M. Mann, *Nature* **2003**, *422*, 198.
[13] P. Roepstorff, J. Fohlman, *Biomed. Mass Spectrom.* **1984**, *11*, 601.
[14] N. G. Rumachik, G. C. McAlister, J. D. Russell, D. J. Bailey, C. D. Wenger, J. J. Coon, *J Am Soc Mass Spectrom* **2012**, *23*, 718.
[15] Y. Liang, P. Neta, X. Yang, S. E. Stein, *J. Am. Soc. Mass Spectrom.* **2018**, *29*, 463.
[16] K. Giles, J. Ujma, J. Wildgoose, S. Pringle, K. Richardson, D. Langridge, M. Green, *Anal. Chem.* **2019**, *91*, 8564.
[17] S. M. Stow, T. J. Causon, X. Zheng, R. T. Kurulugama, T. Mairinger, J. C. May, E. E. Rennie, E. S. Baker, R. D. Smith, J. A. McLean, S. Hann, J. C. Fjeldsted, *Anal. Chem.* **2017**, *89*, 9048.
[18] J. A. Mattocks, J. J. Jung, C.-Y. Lin, Z. Dong, N. H. Yennawar, E. R. Featherston, C. S. Kang-Yun, T. A. Hamilton, D. M. Park, A. K. Boal, J. A. Cotruvo, *Nature* **2023**, *618*, 87.

Manuscript received: May 23, 2025
Revised manuscript received: July 8, 2025
Version of record online: July 30, 2025